

**FABRICATION AND CHARACTERISATION OF
GRAPHENE-POLY (3-HYDROXYBUTYRATE-*co*-
4-HYDROXYBUTYRATE) BIOACTIVE GLASS
COMPOSITE FOR POTENTIAL WOUND
HEALING**

MOHD AIMAN HAKIMI BIN ABD RAHIM

UNIVERSITI SAINS MALAYSIA

2024

**FABRICATION AND CHARACTERISATION OF
GRAPHENE-POLY (3-HYDROXYBUTYRATE-*co*-
4-HYDROXYBUTYRATE) BIOACTIVE GLASS
COMPOSITE FOR POTENTIAL WOUND
HEALING**

by

MOHD AIMAN HAKIMI BIN ABD RAHIM

**Thesis submitted in fulfilment of the requirements
for the degree of
Master of Science**

August 2024

ACKNOWLEDGEMENT

First and foremost, I thank Allah S.W.T for permitting me with health, patience, knowledge, wisdom, and strength to complete this work. Everyone who has carried out research and written a thesis face the challenges and difficulties that come in various forms. It is such a delightful moment to introduce these awesome people who have accompanied me along the journey in this glorious acknowledgement.

A special thanks to Ministry of Higher Education Malaysia who provides Fundamental Research Grant Scheme (FRGS) No. FRGS/1/2018/STG07/USM/02/13 (203.CIPPT.6711664) in supporting the funding of my research work. I would like to express my sincere gratitude to my main supervisor Professor Dato' Dr. Amirul Al-Ashraf Abdullah and co-supervisor Associate Professor Dr. Siti Noor Fazliah Mohd Noor and Associate Professor Ts. Dr. Vigneswari Sevakumaran. Thank you for trusting me, giving freedom to pursue my ideas, and critical supervision to shape my scientific attitude and taught me to view things from different perspectives.

I would like to thank all the staff and student from School of Biological Sciences, staff from Craniofacial & Biomaterial Sciences, staff at Advanced Medical and Dental Institute, Universiti Sains Malaysia for their hard work in assisting me towards completing this research. Special thanks to my family for their support and understanding. Not to mention members of Lab 318 (Jeremy, Julia, Aidda, Hanani, Atikah, Musa, Rozina and Intan), members of Dental Science &AMDI, BOIS USM (Shafiq Nasir, Syafiq Awang, Syauqi, Talha, Basit, Salleh,Shahrul, and Haziq), and H09 communities whom helping me in many ways.

TABLE OF CONTENTS

ACKNOWLEDGEMENT	ii
TABLE OF CONTENTS	iii
LIST OF TABLES	ix
LIST OF FIGURES	xi
LIST OF PLATES	xvi
LIST OF SYMBOLS	xvii
LIST OF ABBREVIATIONS	xviii
LIST OF APPENDICES	xx
ABSTRAK	xxi
ABSTRACT	xxiii
CHAPTER 1 INTRODUCTION	1
1.1 Research Background.....	1
1.2 Problem statement	4
1.3 Objectives of the study	7
1.4 Research Approaches	7
CHAPTER 2 LITERATURE REVIEW	9
2.1 Principles of bioactive materials	9
2.1.1 Properties of bioactive materials	9
2.1.2 Requirement of bioactive materials for regenerative medicine and tissueengineering	10
2.2 Biomaterials in wound healing and skin regeneration application.....	12
2.3 Polyhydroxyalkanoate (PHAs): The next generation biopolymer	20
2.3.1 Derivation of polyhydroxyalkanoate.....	24
2.3.2 Biosynthesis of polyhydroxyalkanoate in microorganisms.....	26
2.3.3 Properties of PHA	30

2.4	Poly(3-hydroxybutyrate-co-4-hydroxybutyrate) [P(3HB-co-4HB)]	31
2.5	Surface modification and functionalisation of biomaterial	33
2.5.1	Modifying the properties of PHA through development of biocomposite	34
2.6	Graphene: The wonder biomaterial	37
2.6.1	Structure and properties of graphene.....	38
2.6.2	Synthesis of graphene	43
2.6.2(a)	Bottom-up methods	44
2.6.2(b)	Top-down methods	46
2.6.3	Development of graphene-based composites towards biomedical application	51
2.7	Bioactive glass (BG) and its structure	53
2.7.1	Properties of bioactive glass.....	56
2.7.2	Synthesis of bioactive glass.....	59
2.7.2(a)	Melt quench method	59
2.7.2(b)	Sol-gel method.....	60
2.7.2(c)	Melt anneal method	62
2.7.3	Modifying the composition of bioactive glass	64
2.7.4	Regenerative properties of bioactive glass	66
CHAPTER 3 MATERIALS AND METHODS		70
3.1	Introduction	70
3.2	General methods.....	72
3.2.1	General drying apparatus	72
3.2.2	Weighing of materials	72
3.2.3	Mixing of materials	72
3.2.4	Sterilisation	72
3.3	Medium preparation	72
3.3.1	Nutrient rich broth	72

3.3.2	Nutrient agar.....	73
3.3.3	Mineral salts medium	74
3.4	Bacterial strain and maintenance of the bacteria.....	75
3.4.1	Microorganism	75
3.4.2	Bacterial stock maintenance.....	76
3.4.3	Seed culture preparation	76
3.5	Biosynthesis of P(3HB- <i>co</i> -4HB) copolymer using fermenter.....	76
3.6	Extraction of P(3HB- <i>co</i> -4HB) copolymer	77
3.7	Removal of endotoxins using oxidising agents.....	78
3.8	Quantification of PHA and its monomer compositions	79
3.8.1	Preparation of methanolysis solution	79
3.8.2	Methanolysis	79
3.8.3	PHA content and the composition of 3HB and 4HB analysis.....	80
3.9	Molecular weight analysis of P(3HB- <i>co</i> -4HB) copolymer	82
3.10	Nuclear magnetic resonance analysis of P(3HB- <i>co</i> -4HB) copolymer	83
3.11	Fabrication of bioactive glass (BG) powder.....	83
3.12	Optimisation and preliminary study of bioactive glass and graphite suspension in the solvent	85
3.12.1	Liquid phase exfoliation of graphite	85
3.12.2	Preparation of bioactive glass suspension.....	86
3.12.3	Preparation of graphite and bioactive glass suspension	86
3.13	Functionalisation of P(3HB- <i>co</i> -4HB)/bioactive glass/graphene composite...	87
3.13.1	Solvent casting of P(3HB- <i>co</i> -4HB) copolymer scaffold.....	87
3.13.2	Solvent casting of P(3HB- <i>co</i> -4HB)/bioactive glass/graphene composite scaffold	88
3.14	Maintenance of cell culture	90
3.14.1	Murine fibroblast (L929) cell lines.....	90
3.14.2	Thawing frozen cells	90

3.14.3	Passaging confluence cells	91
3.14.4	Cell counting and evaluation of viable cells.....	92
3.14.5	Cryopreservation	92
3.14.6	P(3HB-co-4HB) and P(3HB-co-4HB)/bioactive glass/graphene composite scaffolds conditioned medium preparation.....	93
3.15	Characterisation of the P(3HB-co-4HB)/bioactive glass/graphene composite scaffolds	94
3.15.1	Raman spectroscopy analysis.....	94
3.15.2	Fourier transform infrared spectroscopy	95
3.15.3	X-Ray diffraction analysis	95
3.15.4	Differential scanning calorimetry analysis.....	96
3.15.5	pH evaluation	97
3.15.6	Field emission scanning electron microscope (FESEM)	97
3.15.7	Energy dispersive x-ray spectroscopy	98
3.15.8	Atomic force microscopy analysis	98
3.15.9	Hydrophilicity analysis.....	99
3.15.10	Water uptake evaluation of scaffolds	99
3.15.11	Tensile strength analysis	100
3.16	Biocompatibility evaluation and <i>in vitro</i> cytotoxicity test	100
3.16.1	Presto blue assay	100
3.16.2	Field emission scanning electron microscope	102
3.17	Statistical analysis	103
CHAPTER 4 RESULTS.....		105
4.1	Introduction	105
4.2	Biosynthesis of P(3HB-co-4HB) copolymer using 15 L fermenter	106
4.2.1	PHA content and the composition of 3HB and 4HB analysis.....	106
4.2.2	Molecular weight analysis of P(3HB-co-4HB) copolymer	107
4.2.3	Nuclear magnetic resonance (NMR) analysis	108

4.3	Preliminary screening of liquid-phase exfoliation of graphene and bioactive glass.....	111
4.3.1	Optimisation of liquid-phase exfoliation of graphene.....	112
4.3.2	Functionalisation of graphene/bioactive glass suspension in chloroform.....	115
4.4	Fabrication of P(3HB-co-4HB)/graphene/bioactive glass blend scaffold via solvent casting.....	117
4.5	Characterisation of chemical properties of P(3HB-co-4HB)/bioactive glass/graphene blend scaffold.....	119
4.5.1	Fourier transform infrared (FTIR) spectroscopy analysis.....	120
4.5.2	Raman spectroscopy analysis.....	123
4.5.3	X-ray diffraction (XRD) analysis.....	125
4.5.4	pH evaluation study.....	127
4.6	Characterisation of physical and mechanical properties of P(3HB-co-4HB)/bioactive glass/graphene blend scaffold.....	131
4.6.1	Differential scanning calorimetry (DSC) analysis.....	131
4.6.2	Field emission scanning electron microscope (FESEM).....	133
4.6.3	Energy dispersive x-ray spectroscopy (EDX).....	137
4.6.4	Surface topography and roughness analysis.....	139
4.6.5	Surface wettability analysis.....	142
4.6.6	Water uptake evaluation.....	144
4.6.7	Tensile strength analysis.....	147
4.7	Assessment of biocompatibility of P(3HB-co-4HB)/bioactive glass/graphene blend scaffold.....	148
4.7.1	Effects of the cells towards the PHA/BG/G scaffold's extract conditioned medium.....	149
4.7.2	Effects of the cells towards the PHA/BG/G scaffolds upon direct seeding.....	154
CHAPTER 5 DISCUSSION.....		158
5.1	Introduction.....	158

5.2	Pre-formulation and fabrication of P(3HB- <i>co</i> -4HB)/bioactive glass/graphene composite scaffolds	159
5.2.1	Biosynthesis of P(3HB- <i>co</i> -4HB) copolymer <i>via</i> batch fermentation in 15L bioreactor.....	159
5.2.2	Optimisation of graphene-bioactive glass suspension through liquid- phase exfoliation method.....	165
5.2.3	Solvent Casting of P(3HB- <i>co</i> -4HB)/bioactive glass/graphene composite scaffolds	171
5.3	Characterisations of P(3HB- <i>co</i> -4HB)/bioactive glass/graphene composite scaffolds	174
5.3.1	Chemical properties and pH evaluation	174
5.3.2	Physical and mechanical properties.....	181
5.3.3	Biocompatibility and <i>in vitro</i> cytotoxicity assessment.....	193
CHAPTER 6 CONCLUSION AND RECOMMENDATIONS		201
6.1	Conclusion.....	201
6.2	Limitation of this research.....	203
6.3	Recommendation for future research	203
REFERENCES.....		205
APPENDICES		
LIST OF PUBLICATION		

LIST OF TABLES

		Page
Table 2.1	The pros and cons of the various scaffold fabrication techniques used for potential biomedical applications (Adapted from Aiman et al., 2022).....	18
Table 2.2	Characteristics of various types of PHA (Guo et al., 2022).....	30
Table 2.3	Physicochemical properties of graphene (Adapted from Samek et al., 2016)	41
Table 2.4	General properties of sol-gel bioactive glasses (Adapted from Jones & Clare, 2012).....	56
Table 2.5	Effects of the incorporated nickel and cobalt oxide on the mechanical aspects of BG 45S5 (Vyas et al., 2015, 2016).	57
Table 3.1	List of materials that were required in 1.0 L preparation of NR.....	73
Table 3.2	List of materials that were required in 1.0 L preparation of NA.....	73
Table 3.3	List of materials that are required for the preparation of 1.0 L of MSM	74
Table 3.4	List of materials required for the preparation of trace elements in 1.0 L of 0.1 M hydrochloric acid (HCl)	75
Table 3.5	Parameters for PHA analysis in GC	80
Table 3.6	Composition of bioactive glass BG45S5	84
Table 3.7	List of fabricated composite scaffolds	89
Table 3.8	The concentration of ethanol and incubation period for dehydration process.....	103
Table 4.1	Biosynthesis of P(3HB- <i>co</i> -4HB) copolymer in 15 L fermenter	107
Table 4.2	Molecular weight distribution of P(3HB- <i>co</i> -4HB) copolymer	108
Table 4.3	Functional group residue in the composite and control scaffolds	122

Table 4.4	X-ray diffraction studies of P(3HB- <i>co</i> -4HB), bioactive glass, and P(3HB- <i>co</i> -4HB)/3.0 wt.% graphene/2.5 wt.% bioactive glass composite	126
Table 4.5	pH behaviour of PBS solution upon immersion of pure and composite scaffolds	130
Table 4.6	Main thermal properties of the pure and composite scaffolds	133
Table 4.7	Surface roughness of P(3HB- <i>co</i> -4HB) and its composite scaffolds	141
Table 4.8	Water contact angle of P(3HB- <i>co</i> -4HB) and its composite scaffolds	142
Table 4.9	Water absorption of pure and composite scaffold from Day 1 to Day 28	146
Table 4.10	Mechanical properties of the P(3HB- <i>co</i> -4HB) and its composite scaffolds	148

LIST OF FIGURES

	Page
Figure 2.1	The characteristics of engineered scaffold to interact compatibly with biological systems (Adapted from Aiman et al., 2022) 16
Figure 2.2	Chemical structure of PHA. The functional alkyl represents the nomenclature and number of carbons for PHA compound. Asterisk stands for chiral centre for PHA-building block (Adapted from Tan et al., 2014)..... 23
Figure 2.3	Metabolic pathways involved in PHA synthesis (Adapted from Sudesh et al., 2000) 29
Figure 2.4	Chemical structure of P(3HB- <i>co</i> -4HB)..... 33
Figure 2.5	Schematic illustration of graphene σ and π bonds (Adapted from Uran et al., 2017)..... 38
Figure 2.6	Schematic representation of the orbital energy levels of graphene (Adapted from Uran et al., 2017). 39
Figure 2.7	Graphene is a 2D carbon structure; (a) fullerene, (b) carbon nanotubes, (c) graphite (Adapted from Kumar et al., 2019). 40
Figure 2.8	Examples of bottom-up methods to produce graphene a) Chemical vapor deposition; b) Epitaxial growth; c) Arc discharge (Adapted from Moosa & Abed, 2021) 46
Figure 2.9	Illustration of liquid phase exfoliation of graphite and its mechanism (Adapted from Moosa & Abed, 2021) 49
Figure 2.10	Formation of glass based on volume and temperature (Adapted from Paul, 1982) 54
Figure 2.11	(a) Melt quench method, (b) Sol-gel method, and (c) Melt anneal method (Adapted from Dziadek et al., 2016)..... 63
Figure 3.1	Key steps – from product development towards <i>in vitro</i> cell studies..... 71

Figure 3.2	The flow chart of the experimental procedure	71
Figure 3.3	Schematic fabrication of pure P(3HB- <i>co</i> -4HB) scaffolds.....	88
Figure 3.4	Schematic fabrication of pure P(3HB- <i>co</i> -4HB)/BG/graphene composite scaffold	89
Figure 3.5	Heat treatment profile for the DSC.	97
Figure 4.1	¹³ C-NMR spectrum of P(3HB- <i>co</i> -25%4HB) and P(3HB- <i>co</i> -37%4HB) copolymers produced by <i>Cupriavidus malaysiensis</i> USMAA1020	109
Figure 4.2	¹ H-NMR spectrum of control scaffold. (a) P(3HB- <i>co</i> -25%4HB), (b)P(3HB- <i>co</i> -37%4HB)	110
Figure 4.3	UV absorbance intensity of different wight percentage (wt.%) of liquid exfoliated graphene in chloroform at different sonication time from 30 to 180 minutes. (a) 1.0 wt.%, (b) 3.0 wt.%, (c) 6.0 wt.%	113
Figure 4.4	(a) UV absorbance intensity of different weight percentage (wt.%) of liquid exfoliated graphene in chloroform following sonication time at 120 minutes. (b) UV absorbance intensity at 274 to 279 nm at 120 minutes.	114
Figure 4.5	UV absorbance intensity of different weight percentage (wt.%) of bioactive glass suspension in chloroform.	115
Figure 4.6	UV absorbance intensity of liquid exfoliated graphene-bioactive glass suspension in chloroform following 120 minutes sonication time. Different weight percentages of graphite (G) and bioactive glass (BG) used for comparisons as shown in (a) 1.0 wt.%, (b) 3.0 wt.%, (c) 6.0 wt.% of G with 1.0, 2.5, & 5.0 wt.% of BG	116
Figure 4.7	FTIR analysis for P(3HB- <i>co</i> -4HB)/2.5 wt.% bioactive glass/3.0 wt.% graphene blend and control scaffold	121
Figure 4.8	Raman spectra of various scaffolds. Yellow boxes represent bioactive glass spectrum whereas red boxes represent pure P(3HB- <i>co</i> -4HB) spectrum	124

Figure 4.9	XRD analysis for P(3HB- <i>co</i> -4HB), bioactive glass, and P(3HB- <i>co</i> -4HB)/3.0 wt.% graphene/2.5 wt.% bioactive glass composite. The symbols (*) and (#) refer to Na ₂ Ca ₂ Si ₃ O ₉ and Na ₂ Ca ₃ Si ₆ O ₁₆ , respectively	126
Figure 4.10	pH behaviour of PBS solution upon immersion of pure and composite scaffolds	129
Figure 4.11	DSC curves (second scan) of (a) P(3HB- <i>co</i> -37%4HB) pure polymer, and (b) P(3HB- <i>co</i> -37%4HB)/3.0 wt.% graphene/2.5 wt.% bioactive glass composite	132
Figure 4.12	Scanning electron micrograph of P(3HB- <i>co</i> -4HB) and composite scaffolds observed under 500X magnification. (a) P(3HB- <i>co</i> -25%4HB), (b) P(3HB- <i>co</i> -37%4HB), (c) P(3HB- <i>co</i> -25%4HB)/3.0 wt.% graphene/2.5 wt.% bioactive glass, (d) P(3HB- <i>co</i> -37%4HB)/3.0 wt.% graphene/2.5 wt.% bioactive glass	135
Figure 4.13	Scanning electron micrograph of P(3HB- <i>co</i> -4HB) composite scaffolds observed under 1000X magnification. (a) P(3HB- <i>co</i> -25%4HB)/3.0 wt.% graphene/2.5 wt.% bioactive glass, (b) P(3HB- <i>co</i> -37%4HB)/3.0 wt.% graphene/2.5 wt.% bioactive glass	136
Figure 4.14	The EDX profile is shown for (a) P(3HB- <i>co</i> -25%4HB), (b) P(3HB- <i>co</i> - 37%4HB), (c) P(3HB- <i>co</i> -25%4HB)/3.0 wt.% graphene/2.5 wt.% bioactive glass, (d) P(3HB- <i>co</i> -37%4HB)/3.0 wt.% graphene/2.5 wt.% bioactive glass.....	138
Figure 4.15	AFM images of surface topography of tested scaffolds. The surface roughness is represented by two-dimensional image (right) and three-dimensional image (left). (a) P(3HB- <i>co</i> -25%4HB); (b) P(3HB- <i>co</i> -37%4HB); (c) P(3HB- <i>co</i> -25%4HB)/3.0 wt.% graphene/2.5 wt.% bioactive glass; (d) P(3HB- <i>co</i> -37%4HB)/3.0 wt.% graphene/2.5 wt.% bioactive glass.....	140
Figure 4.16	Water contact angle measurement of (a) P(3HB- <i>co</i> -25%4HB); (b) P(3HB- <i>co</i> -37%4HB); (c) P(3HB- <i>co</i> -25%4HB)/3.0 wt.% graphene/2.5 wt.% bioactive glass; (d) P(3HB- <i>co</i> -37%4HB)/3.0 wt.% graphene/2.5 wt.% bioactive glass.....	143

Figure 4.17	Water uptake evaluation of pure P(3HB- <i>co</i> -4HB) and P(3HB- <i>co</i> -4HB)/3.0 wt.% graphene/2.5 wt.% bioactive glass scaffolds	145
Figure 4.18	Cell proliferation of seeded murine fibroblast cell (L929) using Presto Blue that were performed at various dosage on P(3HB- <i>co</i> -25%4HB) and P(3HB- <i>co</i> - 25%4HB)/3.0 wt.% graphene/ 2.5 wt.% bioactive glass. Means data accompanied by different alphabet indicates significant different within the group at $P \leq 0.05$ level (Tukey test). Refer Appendix I Post hoc of one-way ANOVA analysis was performed separately for each pure and composite scaffold-conditioned medium.	150
Figure 4.19	Cell proliferation of seeded murine fibroblast cell (L929) using Presto Blue that were performed at various dosage on P(3HB- <i>co</i> -37%4HB) and P(3HB- <i>co</i> - 37%4HB)/3.0 wt.% graphene/ 2.5 wt.% bioactive glass. Means data accompanied by different alphabet indicates significant different within the group at $P \leq 0.05$ level (Tukey test). Post hoc of one-way ANOVA analysis was performed separately for each pure and composite scaffold-conditioned medium.....	151
Figure 4.20	Cell proliferation of seeded murine fibroblast (L929) cells using Alamar Blue that were performed at Day 1, 4, 7, 14, 21, and 28 on P(3HB- <i>co</i> -4HB), P(3HB- <i>co</i> -4HB)/3.0 wt.% graphene/ 2.5 wt.% bioactive glass (5.00 and 10.00 mg/ml). Means data accompanied by different alphabet indicates significant different within the group at $P \leq 0.05$ level (Tukey test). Refer Appendix J	153
Figure 4.21	Cell proliferation of seeded murine fibroblast (L929) cells using Presto Blue assay that were performed at Day 1, 4, 7, 14, 21, and 28 on P(3HB- <i>co</i> -4HB), P(3HB- <i>co</i> -4HB)/3.0 wt.% graphene/ 2.5 wt.% bioactive glass. Means data accompanied by different alphabet indicates significant different within the group at $P \leq 0.05$ level (Tukey test). Refer Appendix K	156

Figure 4.22 SEM micrograph of proliferation of murine fibroblast (L929) cells on P(3HB-co-37%4HB)/3.0 wt.% graphene/ 2.5 wt.% bioactive glass. (a) 500X magnification (b) 1000X magnification 157

LIST OF PLATES

	Page
Plate 4.1	Copolymer film of P(3HB- <i>co</i> -4HB) (a) P(3HB- <i>co</i> -37%4HB), and (b) P(3HB- <i>co</i> -25%4HB) 118
Plate 4.2	P(3HB- <i>co</i> -4HB)/3.0 wt.% graphite/2.5 wt.% bioactive glass blend scaffold. The different types of scaffolds represented (a) P(3HB- <i>co</i> -37%4HB) and (b) P(3HB- <i>co</i> -25%4HB) 119
Plate 4.3	P(3HB- <i>co</i> -4HB)/6.0 wt.% graphite/2.5 wt.% bioactive glass blend scaffold. The different types of scaffolds represented (a) P(3HB- <i>co</i> -37%4HB) and (b) P(3HB- <i>co</i> -25%4HB) 119

LIST OF SYMBOLS

%	Percentage
°	Degree
θ	Incidence Angle of X-Ray Beam
°C	Degree Celsius
μm	Micrometer
g	Gram
<i>g</i>	Gravity
g/mol	Gram per mole
mol.%	Mol percentage
MPa	Mega pascal
psi	Pound per square inch
Ra	Average roughness
Rmax	Maximum roughness depth
rpm	Rotations per minute
Rq	Root mean square roughness
v/v	Volume per volume
vvm	Gas volume flow per unit of liquid volume per minute (volume per volume per minute)
w/v	Weight per volume
wt.% C	Weight percentage of carbon
wt.%	Weight percentage

LIST OF ABBREVIATIONS

^{13}C -NMR	Carbon-Nuclear Magnetic Resonance
^1H -NMR	Proton-Nuclear Magnetic Resonance
AFM	Atomic Force Microscopy
ANOVA	Analysis of Variance
ASTM	American Society for Testing Materials
ATCC	American Type Culture Collection
ATR	Attenuated Total Reflectance
BG	Bioactive Glass
BO	Bridging Oxygen
C	Carbon Atom
C=O	Carbonyl
CME	Caprylic Methyl Ester
CoA	Coenzyme A
DO	Dissolved Oxygen
DPBS	Dulbecco's Phosphate Buffered Saline
DSC	Differential Scanning Calorimetry
ECM	Extracellular Matrix Mineralisation
EDX	Energy Dispersive x-ray Spectroscopy
FESEM	Field Emission Scanning Electron Microscopy
FTIR	Fourier Transform Infrared Spectroscopy
GC	Gas Chromatography
GPC	Gel-Permeation Chromatography
HA	Hydroxyapatite
HCA	Hydroxyl Carbonate Apatite

kDa	Kilo Dalton
MCL	Medium Chain Length
MEM	Minimum Essential Medium
<i>M_n</i>	Number-average Molecular Weight
<i>M_w</i>	Weight-average Molecular Weight
NBP	Non-bridging Oxygen
N _c	Network CONNECTIVITY
NMR	Nuclear Magnetic Resonance
OD	Optical Density
PB	Presto Blue
PBS	Phosphate Buffer Saline
PBS	Phosphate Buffered Saline
PDI	Polydispersity Index
PhaA	β-kethiolase
PhaB	Acetoacetyl-CoA Reductase
PhaC	PHA Synthase
PhaG	(R)-3-hydroxyacyl-ACP-CoA-transferase
PhaJ	(R)-specific-enoyl- CoA hydratase
PhaP	Phasin
PhaR	Regulator PROTEIN for Phasing Expression
PhaZ	PHA Depolymerase
PTFE	Polytetrafluoroethylene
T _c	Crytsallisation Temperature
T _g	Glass Transition Temperature
T _m	Melting Temperature
XRD	X-ray Diffraction

LIST OF APPENDICES

- Appendix A Set-up for Techfors-S 15L and the main components
- Appendix B Statistical analysis for GC analysis using SPSS statistics software version 27
- Appendix C Statistical analysis for GPC analysis using SPSS Statistics Software Version 27
- Appendix D Statistical analysis for pH evaluation using SPSS Statistics Software Version 27
- Appendix E Statistical analysis for AFM analysis using SPSS Statistics Software Version 27
- Appendix F Statistical analysis for water contact angle analysis using SPSS Statistics Software Version 27
- Appendix G Statistical analysis for water uptake analysis using SPSS Statistics Software Version 27
- Appendix H Statistical analysis for tensile strength analysis using SPSS Statistics Software Version 27
- Appendix I Statistical analysis for Presto Blue analysis (Dosage study) analysis using SPSS Statistics Software Version 27
- Appendix J Statistical analysis for Presto Blue analysis (5.00 and 10.00 mg/ml) analysis using SPSS Statistics Software Version 27
- Appendix K Statistical analysis for Presto Blue analysis (Cells seeded on scaffolds) using SPSS Statistics Software Version 27

**PEMFABRIKATAN DAN PENCIRIAN GRAFEN-POLI (3-
HIDROKSIBUTIRAT-KO-4-HIDROKSIBUTIRAT) KACA AKTIF BIO
KOMPOSIT UNTUK POTENSI PENYEMBUHAN LUKA**

ABSTRAK

Mengurus luka secara klinikal merupakan cabaran yang ketara. Ia melibatkan tidak hanya memastikan pembalutan menyediakan penghalang yang diperlukan dan menggalakkan penyembuhan tetapi juga memerlukan pertimbangan kepatuhan pesakit dari segi keselesaan, fungsi, dan praktikaliti. Poli(3-hidroksibutirat-*ko*-4-hidroksibutirat) merupakan biopolimer yang berasal dari bakteria dan terkenal kerana sifat kimia, fizikal, dan mekanikal yang menarik. P(3HB-*ko*-4HB) dikenali secara meluas sebagai bahan yang boleh terbiodegradasi dan sangat biokompatibel. Namun, kopolimer P(3HB-*ko*-4HB) mempunyai hadnya kerana ia menunjukkan sifat hidrofobik, sehingga menyekat potensinya dalam perubatan regeneratif. Penambahbaikan bahan boleh menangani kekangan tertentu dalam matriks polimer, seperti hidrofisiliti, tingkah laku mekanikal, dan struktur morfologi serta biokompatibiliti. Dalam mencapai matlamat ini, kaca bioaktif dan grafen telah digabungkan ke dalam struktur perancah untuk meningkatkan ciri-ciri fisiko-kimia kopolimer P(3HB-*ko*-4HB). Kaca bioaktif (BG) dikenali kerana keupayaannya untuk merangsang vaskularisasi dan mengawal molekul anti-radang dan faktor pertumbuhan semasa pelepasan ionnya, yang mana ia akan meningkatkan proses penyembuhan luka. Grafen diketahui mempunyai sifat elektrik, mekanikal, termal, kimia yang sangat baik, dan luas permukaan yang tinggi. Ia disintesis menggunakan teknik pengelupasan fasa cecair, yang merupakan pendekatan yang boleh dipercayai untuk mendapatkan grafen berkualiti tinggi dan ekonomik. Dalam projek ini, penghasilan komposit polimer telah

dioptimumkan dan dijelaskan menggunakan pelbagai aspek penjelmaan kimia, fizikal, dan mekanikal. Peningkatan lanjutan komposit melalui penambahan kaca bioaktif dan grafen yang diekfoliasi secara cecair juga telah disiasat. Biokompatibiliti komposit telah dinilai menggunakan sel fibroblas murin (L929). Secara ringkasnya, P(3HB-*ko*-4HB) berjaya dipisahkan dari bakteria dengan profil fisiko-kimia yang ditakrifkan bergantung pada prekursor karbon. Peningkatan tambahan kopolimer dengan kaca bioaktif dan grafen menghasilkan peningkatan nilai (hingga pH 8) disebabkan oleh pelepasan ion dari BG yang berkolerasi dengan mekanisme hidroksi karbonat apatit (HCA), yang merangsang proses penyembuhan luka. Perancah komposit mengakibatkan peningkatan kekasaran permukaan dengan pembentukan liang tidak teratur dan protuberans. Kekasaran dan kapasiti penyerapan air meningkat selepas penambahan 3.0 wt.% grafen dan 2.5 wt.% kaca bioaktif sementara tiada kesan merosakkan dari segi termal dan mekanikal. Sel fibroblas L929 juga menunjukkan kesan positif dari segi biokompatibiliti semasa 14 hari inkubasi. Kajian ini menekankan kepentingan mengoptimumkan setiap bahan dalam komposit dan interaksi mereka dalam menyesuaikan ciri-ciri bahan. Kemajuan ini dalam penampalan luka membantu memudahkan penyembuhan luka dan mempunyai potensi dalam regenerasi tisu berpandu.

**FABRICATION AND CHARACTERISATION OF GRAPHENE-
POLY(3-HYDROXYBUTYRATE-*CO*-4-HYDROXYBUTYRATE)
BIOACTIVE GLASS COMPOSITE FOR POTENTIAL WOUND HEALING**

ABSTRACT

Managing wounds clinically presents a notable challenge. It involves not only ensuring that the dressing provides necessary barrier and promotes healing but also requires consideration of patient compliance in term of comfort, functionality, and practicality. Poly(3-hydroxybutyrate-*co*-4-hydroxybutyrate) is a bacterial derived biopolymer widely notable for its exceptional chemical, physical, and mechanical properties. P(3HB-*co*-4HB) is widely known to be biodegradable and highly biocompatible. However, P(3HB-*co*-4HB) copolymer has its limitation as it exhibits hydrophobic properties, thus restrict its potential in regenerative medicine. Improving materials can address specific limitations within polymer matrices, such as hydrophilicity, mechanical behaviour, and morphological structure as well as biocompatibility. In pursuit of this goal, bioactive glass and graphene were integrated into the scaffold to enhance the physicochemical characteristics of the P(3HB-*co*-4HB) copolymer. Bioactive glass (BG) is recognised for its ability to stimulate vascularisation and regulate anti-inflammatory molecules and growth factor upon the release of its ions, which on turn enhances the process of wound healing. Graphene is known to possess excellent electrical, mechanical, thermal, chemical properties, and high surface area. It was synthesised using the liquid-phase exfoliation technique, which is a dependable approach for obtaining high quality graphene and economically viable. In this project, the fabrication of the polymeric composite was optimised and described using a range of chemical, physical, and mechanical characterisation

aspects. The further enhancement of the composite through addition of bioactive glass and liquid-exfoliated graphene was also investigated. The biocompatibility of the composite was assessed using murine fibroblast (L929) cells. In short, P(3HB-co-4HB) was successfully isolated from the bacteria with the defined physico-chemical profiles dependent on the carbon precursors. The additional enhancement of the copolymer with bioactive glass and graphene resulted in increment in its value (up to pH 8.0) due to ion release from BG correlated with the hydroxy carbonate apatite (HCA) mechanism, which induce wound healing process. Composite scaffolds lead to increase in surface roughness with formation of irregular pores and protuberances. Wettability and water uptake capacity increased following the incorporation of 3.0 wt.% graphene and 2.5 wt.% bioactive glass while no detrimental effects in terms of thermal and mechanical. The L929 fibroblast cells also show positive effect in term of biocompatibility during 14 days of incubation. This study highlights the significance of optimising each material within the composite and their interplay in fine-tuning the materials properties. This advancement of wound patch help to facilitate wound healing and have potential in guided tissue regeneration.

CHAPTER 1

INTRODUCTION

1.1 Research Background

Biomaterials are bioactive material that can trigger a biological response at the surface of the materials by structuring specific bonds between the tissues and material itself (Cao & Hench, 1996). Currently, biopolymers provide significant advantages of having capability to be degrade after its intended role and slowly withdraw thereafter. Compared to conventional chemical-based polymers, bio-sourced polymers show various advantages and are usually synthesised from economical and renewable resources as well. Moreover, biopolymer's excellent biological properties and degradability allow them to be widely utilised as biomaterial scaffolds (Yu et al., 2021). Biopolymer scaffold has been engineered to connect with our biological system in contributing three-dimensional (3D) structure and mimicking an extracellular matrix (ECM). Furthermore, biopolymer is known to interact with surrounding cells of tissues constructing a regenerative ecosystem, a process known as tissue engineering (TE). Therefore, continuous research is focusing to design biologically active scaffolds with considerable interlinked configuration and surface chemistry to maximise its cellular interaction on the scaffold interface whilst inducing wound healing response.

Polyhydroxyalkanoates (PHA) is well known for their excellent biocompatibility and tailorable retention rate, making them the preferred biopolymer for tissue engineering (Możejko-Ciesielska & Kiewisz, 2016). PHA are linear polyesters that are massed in cell cytoplasm as energy reserve compounds which are

produced by bacterial microbiomes, under stress conditions (Salim et al., 2012; Trakunjae et al., 2021; Winnacker, 2019). Among the various microorganisms, Gram-negative bacteria for instance *Cupriavidus*, *Bukholderia*, and *Azohydromonas*. Not to mention, Gram-positive bacteria also has the capacity to synthesise PHA such as *Bacillus*, *Corynebacterium*, *Clostridium*, *Caryophanon*, *Micrococcus*, *Microlunatus*, *Microcystis*, *Nocardia*, *Rhodococcus*, *Staphylococcus*, and *Streptomyces* (Tan et al., 2014). It is one of the most promising biopolymers as they are totally biodegradable, biocompatible, and retains properties, which closely resemble to synthetic thermoplastics (Anderson & Dawes, 1990). Besides, this bacterial-derived biopolymer has intrigued great spotlights in the biomedical application due to their exceptional properties such as biocompatibility and biodegradability, which are not achievable in the existing synthetic polymers (Bordes et al., 2009; Sudesh et al., 2000). Since it exhibits excellent biodegradability, PHA is progressing as the dynamic material due to their chemical variation and produced from sustainable carbon sources (Tan et al., 2014).

Among the various PHAs, poly(3-hydroxybutyrate-*co*-4-hydroxybutyrate) P(3HB-*co*-4HB) copolymer is an emerging biopolymer with interesting properties in biomedical applications due to the non-toxic byproducts, versatility in physical and mechanical properties, non-carcinogenic side effects, and biocompatibility (Faedah et al., 2011). P(3HB-*co*-4HB) has Food and Drug Administration (FDA) approval for clinical practices among the rest PHAs available (Vigneswari et al., 2020). This copolymer was biosynthesised by bacterium *Cupriavidus necator* (previously *Ralstonia eutropha*) from structurally related carbon sources such as γ -butyrolactone and 4-hydroxybutyric acid (Faedah et al., 2011; Salim et al., 2012). This copolymer

also exhibits a wide range of structures which comprises of highly crystalline (brittle) monomer 3HB and elastomeric rubber-like (ductile) monomer 4HB.

Bioactive glass (BG) has been proposed in biomedical following the success of bioactive glass cones as middle ear prosthesis in human (Rust et al., 1996). BG has been extensively applied in tissue engineering applications due to its biodegradability which aiding many treatment approaches. There are variety of bioactive glasses that are available from silicate-based, borate-based and phosphate-base (Fatimah et al., 2020). Bioactive glass is categorised as Class A biomaterial which could configure bonds with both soft and hard tissues. 45S5 Bioglass[®] is the first fabricated BG by Professor Hench in 1969 that having composition of 46.1% SiO₂, 26.9% CaO, 24.4% Na₂O and 2.5% P₂O₅ (mole percentages, mol.%) (Cao & Hench, 1996). In term of bioactivity, BG is known to be osteoinductive which promotes the repair and regeneration of both soft and hard tissues via deposition of bioactive layer of hydroxyapatite (HA) and hydroxylcarbonate apatite (HCA) over its surface (Kokubo & Takadama, 2006).

Further, the next bioactive material to be incorporated in the composite is the well-known wonder material, graphene. Graphene has grabbed the attention of many researchers as for becoming a new wonder material in science and technology as well as an exciting new topic in the field of carbon nanoscience in recent years. Naturally, graphene consists of a single thick planar two-dimensional (2D) sheet that exhibits honeycomb or hexagonal lattice structure which comprises of sp² hybridised carbon atoms family (Novoselov et al., 2004). It possesses great potential towards biomedical applications, which trigger the interaction with cellular components such as DNA, membranes, and proteins (Fan et al., 2010; Singh et al., 2018). After the success of its exfoliation, graphene has become one of the most appealing materials for its properties

such as good electric and thermal conductivity, and biocompatible with the cells which are highly desirable for scaffold material in tissue engineering application.

Interestingly, graphene also known to function as photothermal agent with high near- infrared region (NIR) absorbing properties that can stimulate cellular processes (Pinheiro et al., 2002). This stimulatory effect has shown improvement on mitochondria activity which resulting increase in adenosine triphosphate (ATP) (Hourelid, 2014).

1.2 Problem statement

Rapid bleeding control and efficient wound healing are crucial components of medical care as emergencies are still the leading cause of early death worldwide. However, serious trauma that results in uncontrolled bleeding and healing difficulties is linked to a high fatality rate (Hong et al., 2019; Zia et al., 2020). The World Health Organisation (WHO) estimates that annually, burns result in 180 000 fatalities and more than 11 million cutaneous wounds necessitate prompt and adequate medical care (Monavarian et al., 2019). The market for wound care products is anticipated to be valued at USD15–22 billion (Dollar United States) in 2024 because of the extensive research done and the high demand for dressing materials, which make most resorbable wound patch in the market is expensive (Raju et al., 2022). Currently, gauzes are suboptimal choices for wound dressing due to their potential to induce trauma and mechanical irritation during removal, leading to increased patient discomfort. Additionally, they may leave behind residues such as fibres or particles, which can trigger immune responses and contribute to the formation of granulomas (Sood et al., 2014).

There is need in the exploration and optimisation of wound patches to achieve effectiveness in promoting wound healing through investigating novel combinations of biomaterials, such as incorporating natural polymers and bioactive agents to develop composite materials. The importance of understanding on how specific material properties such as surface topography, porosity, degradation rate, and bioactivity, influence cellular responses and tissue regeneration in wound healing contexts. This involves fine-tuning material properties to better mimic the native extracellular matrix (ECM) and create an optimal microenvironment for wound repair. By addressing these research gaps, the development of scaffolds for wound healing ultimately leading to improved clinical outcomes and quality of life for patients with chronic and acute wounds.

Meanwhile, modern wound dressings need to mimic the natural environment to promote cell adhesion and proliferation at a specific site. These substances ought to be permeable in nature. High porosity dressings will promote cell migration, proliferation, and efficient delivery of nutrients, active ingredients, oxygen, and metabolites to and from the site of regeneration. The selection of a suitable biomaterial is important in developing functional scaffold which provides the surface architecture and mechanical support for the proliferation of cells. Although there are several chances for biopolymer modification, excessive modification may undermine the material's inherent biological capabilities, hence it is important to consider an appropriate alteration (Qin et al., 2022).

The development of dressing materials using biocompatible polymers, such as polyhydroxyalkanoates (PHAs), may be a great way to increase patient comfort. This is since these polymers are completely resorbable, eliminating the need to change the

dressing. Although exhibiting many advantageous properties, P(3HB-*co*-4HB) is not bioactive as it lacks functional sites for cell attachment and poor hydrophilicity, which restricts the applications for wound healing. Therefore, the main strategies proposed to tackle this limitation is the incorporation with bioactive and inorganic materials, and among them, bioactive glass (BG) and graphene have been the focus of this study.

Following the aforementioned background, an innovative approach whereby biocompatible polymers can be fine-tuned with the ionic released from bioactive glass and graphene as a photothermal agent to enhance wound healing process. In term of reducing the cost of production, production of raw materials including P(3HB-*co*-4HB), graphene, and bioactive glass are economical, focusing on the optimisation of liquid-phase exfoliation of graphite. Plus, combination of biopolymer with bioactive glass and graphene which can be applied into use after assessing their characteristics. If the study verifies to be a success, these P(3HB-*co*-4HB)/bioactive glass/graphene composite scaffold can be commercially proposed and imposed to and subsequently implemented in soft tissue healing and regeneration.

In this study, focused are aimed towards the application of P(3HB-*co*-4HB) copolymer, bioactive glass, and graphene composite scaffold in wound healing. The aim is to maintain the hydration and gas exchange within the wound gap, easy application and painless removal, and act as a barrier to external pathogen to the surrounding skin for reducing inflammation and encouraging fibroblast proliferation for skin renewal with minimal exudate (Yao et al., 2015). The combination of P(3HB-*co*-4HB), bioactive glass, and graphene scaffolds fabricated through solvent casting method and their characteristics were assessed. Hence, the current study aspiration was to explore the effect of bioactive glass and graphene combined with P(3HB-*co*-4HB)

and characterise the chemical, physical, and mechanical properties. The *in vitro* biological assessment is performed towards the murine cell line to confirm its potential use in wound healing for soft tissue regeneration.

1.3 Objectives of the study

The general objective of this research is to develop P(3HB-*co*-4HB)/bioactive glass/graphene composites scaffolds through solvent casting method.

The specific objectives of the study include:

- i. To biosynthesise P(3HB-*co*-4HB) copolymer through fermentation process using 15 L bioreactor.
- ii. To perform graphene exfoliation through liquid-phase exfoliation (LPE) method.
- iii. To fabricate and characterise P(3HB-*co*-4HB)/bioactive glass/graphene composites and evaluate its biocompatibility towards murine fibroblast (L929) cells using Presto Blue assay.

1.4 Research Approaches

The P(3HB-*co*-4HB) as the biopolymer of interest was synthesised through batch fermentation using wild type *Cupriavidus malaysiensis* USMAA1020 with the addition of carbon precursor, later the crude polymer was extracted by a series of process using chloroform and methanol. The crude P(3HB-*co*-4HB) copolymer was characterised using gas chromatography and gel-permeation chromatography. The bioactive glasses based on quaternary system of SiO₂-CaO-Na₂O-P₂O₅ were fabricated using sol-gel method, while graphene nanoparticles were exfoliated from graphite powder using liquid-phase exfoliation method. The exfoliation of graphene and

bioactive glass/graphene suspension were optimised using UV-Vis spectroscopy. The P(3HB-*co*-4HB) biopolymer and bioactive components bioactive glass and graphene were fabricated using solvent casting method.

The P(3HB-*co*-4HB)/bioactive glass/graphene composites scaffolds were subjected to characterisation including chemical, physical, and mechanical evaluations. The composite and pure scaffolds were characterised using Fourier transform infrared (FTIR) spectroscopy analysis, Raman spectroscopy analysis, nuclear magnetic resonance (NMR) analysis, x-ray diffraction (XRD) analysis, and pH evaluation study. Then, the composites and pure scaffolds were subjected to physical and mechanical characterisation using differential scanning calorimetry (DSC) analysis, field emission scanning electron microscope (FESEM), energy dispersive x-ray spectroscopy (EDX), atomic force microscopy (AFM) analysis, water contact angle analysis, water uptake evaluation, and tensile strength analysis.

The biocompatibility of P(3HB-*co*-4HB)/bioactive glass/graphene composites scaffolds was assessed using composite-conditioned medium with different weight to liquid ratio towards murine fibroblast (L929) cells using Presto Blue assay at 48 hours for determining the optimum dose. Later, the pre-screened weight to liquid ratio were incubated at various time intervals (Days 1, 4, 7, 14, 21, 28). Moreover, the selected composite scaffold was viewed under field emission scanning electron microscope (FESEM) to observe cell attachment onto the scaffold.

CHAPTER 2

LITERATURE REVIEW

2.1 Principles of bioactive materials

2.1.1 Properties of bioactive materials

A biomaterial's primary purpose is to replace tissues that have been harmed or are diseased. Bioactivity describes the properties of a substance that can form bonds with the host tissues. According to the definition of bioactive materials, they are substances that can cause a specific biological reaction at their interface as a result of the bonds they form with living tissues (Polymeris et al., 2017). Currently, substantial research is being done on biomaterials for commercialisation and application, particularly for biological applications.

Generally, biomaterials for regenerative medicine application are classified into bioinert and bioactive materials. The term "bioinert" describes any material that, when ingested into a human body, interacts with the tissue only slightly (Rao et al., 2022). Bioinert materials refer to materials with slow degradation rates, temporary support and similar properties to skin tissue including artificial skin grafts (Tan et al., 2021). For example, metals (titanium and cobalt-chrome-based alloys), ceramics (alumina and zirconia), silicone rubber, and acrylic resins. A bioactive material is described as one that causes a certain biological reaction at its interface and causes a bond to form between the tissue and the substance, by creating extracellular and intracellular reaction (Rao et al., 2022). Then, the focus is the bioactive materials, which able to stimulate and facilitate skin tissue regeneration by providing supportive scaffolds and stimulatory factors for cells to attach to, proliferate and differentiate (Pina et al., 2019).

2.1.2 Requirement of bioactive materials for regenerative medicine and tissue engineering

Regenerative medicine is a transdisciplinary field composing of engineering materials, medical devices, artificial organ, and cellular therapies which hold the promise of repairing and replacing tissues damaged by injuries or diseases. The aim is to treat or cure those missing tissues by effectively replenishing it both structurally and functionally to contribute to tissue healing. using body's own regenerative capabilities. Tissue engineering has propelled the concept of regenerative medicine into promising reality by the emulation of cell-extracellular matrix dynamic interplay in the healthy natural tissues, which will be used to artificially develop substitutes for tissue repair and replacement therapies (Mao & Mooney, 2015). Development of bioactive material is important for regenerative medicine and tissue engineering applications which cells are strictly required to grow and perform its function appropriately, which further preserve new extracellular matrix to configure new tissue and capable to perform sophisticated organ system.

Due to their distinct qualities, biologically active natural materials have gained popularity to be employed as possible materials in tissue engineering. Their physical and chemical similarity makes them able to mimic the structure of human tissue, which activate induced tissue regeneration from cells with the assist of biomaterials and bioactive components (Aiman et al., 2022; Yun, 2015). Bioactive material is selected based on chemical and mechanical of the specific biological system to achieve desired functional outcome. Each of these aspects offers specific advantages which can be suitably employed to stimulate the microenvironmental conditions of targeted tissue. To be effective biomaterial in tissue engineering, the materials should possess fundamental properties such as: (1) biocompatibility with tissues; (2) a

biodegradability rate that is correspond to the pace at which new tissue is formed; (3) nontoxicity and nonimmunogenicity; (4) optimum mechanical properties; and (5) an adequate morphology for transporting cells, gases, metabolites, nutrients, and signal molecules both inside and outside of the host environment's materials (Stratton et al., 2016). Bioactive materials play diverse roles in regenerative medicine including scaffold development for tissue engineering, drug delivery systems, biodegradable implants, biomimetic surfaces, and stem cell therapy. In term of scaffold development, several advantages were reported as bioactive material provide structural support and guide tissue regeneration as they mimic the native environment of cells.

Tissue engineering uses a wide range of bioactive materials based on metals, polymers, ceramics, and their composites. Bioactive devices constructed from biodegradable materials based on natural polymers have advantages as degraded biomaterial does not require second clinical surgery to remove the implanted wound dressing when the damaged tissue heals completely. Due to their outstanding biocompatibility, degradability, and cell-cell recognition capacities, natural biopolymer such as PHA are widely used in the biomedical and pharmaceutical industries. Meanwhile, the diverse forms of inorganic-based biomaterials are suitable candidate for tissue engineering. They provide the benefits of high bioactivity, good biocompatibility, blood absorption, blood coagulation stimulation, and release of bioactive ions (Dalisson & Barralet, 2019). However, these active inorganic components have few limitations such as uncontrolled degradation, poor mechanical properties, difficulties in bioaccumulation of degradation products, and local acidic environments. In term of degradation rate, it may vary depending on factors such as implant location, surrounding tissue environment, and patient specific factors. This will affect the stability and longevity of the scaffold, impacting its effectiveness in

promoting tissue regeneration. While bioactive material is generally biocompatible, individuals may encounter adverse reactions from interactions between the material and the body's tissues. It could lead to complication like infection, inflammation, or fibrosis. These drawbacks do not meet the requirements for tissue engineering (Islam et al., 2020). Thus, an effort is crucial to overcome these challenges by developing hybrid bio-composites with superior properties. Surface functionalisation approach by incorporating bioactive molecules or coatings to the material's surface helps to improve cell adhesion, proliferation, and differentiation. Combination of biopolymer with inorganic materials able to reduce the limitations of single-component materials. These modifications aim to tailor bioactive materials to specific regenerative medicine applications, improving their performance and therapeutic potential in promoting tissue repair and regeneration.

2.2 Biomaterials in wound healing and skin regeneration application

Skin plays a key role in protecting internal environment from external threats, maintaining homeostasis, and regulating temperature. It is composed of epidermis on the outer side and inner dermis layer; each layer with specific functions, such as prevention of dehydration, a barrier to refrain trauma, sensory perception, synthesis of vitamin D, and immune control (Ibrahim et al., 2021). The outer layer of epidermis consists generally of keratinocytes, which eventually proliferate from the basal layer and differentiate at the terminal layer of the epidermis (Ibrahim et al., 2021). Concurrently, complex nature of skin makes it particularly difficult to imitate in the laboratory which makes wound healing becoming a vital process. The healing process consisting of four overlaying and systematic stages including: (1) an inflammatory stage characterised by macrophage or leucocytes infiltration and cytokine production; (2) a proliferative phase which includes removal of damaged tissue and formation of

granulation tissue in the wound; (3) a maturation phase where extracellular matrix generated by the proliferative tissue becomes well-defined; and (4) the formation of scar tissue demonstrating the completion of the wound healing process, which keratinocytes migrate to reseal the skin (Schilrreff & Alexiev, 2022).

Biomaterials are the backbone of scaffolds, and it is the main character to play role in the functions of the scaffolds. According to the National Science Foundation workshop, among the current innovations in the multidisciplinary of wound regenerative medicine, scaffolds are the best materials for restoring, maintaining, and improving tissue function (Ehrenreich & Ruszczak, 2006; Tottoli et al., 2020). They play a particular role in repair and regeneration of tissues by providing a suitable platform, permitting necessary supply of various factors related with continuity, proliferation, and differentiation of cells. For instance, polymeric composite scaffold from a combination of poly(lactic-*co*-glycolic acid) (PLGA) and collagen, which have the ability to support cell growth, degrade safely as wound heals, and can be adjusted to fit different needs (Guzman-Soria et al., 2023). The composition and properties of the composites can be tailored by adjusting the ratio of both components, controlling scaffold porosity, or modifying scaffold architecture through techniques like electrospinning or 3D printing. Then, commercial scaffold known as Integra™ consist of poly(glycolic acid) (PGA), collagen, and glycosaminoglycan which mimics the extracellular matrix of human skin. Due to its porous structure, it allows for the infiltration of cells while the collagen layer promotes cell proliferation. As the wound heals, the polymer gradually degrades. In term of clinical application, Integra is used to treat severe burns and wounds. It helps heal wounds, reduce scars, and restore the function of the skin (Melendez et al., 2008).

However, in some cases improper scaffold selection or design can result in delayed wound healing or incomplete tissue regeneration, prolonging the recovery process for the patient. Plus, inadequate scaffold design or modification led to excessive scarring and keloid formation. These issues will negatively impacting the cosmetic appearance and functionality of the regenerated skin. Addressing these disadvantages requires consideration of scaffold material selection and design optimisation to ensure successful skin regeneration and minimise complications.

The development of wound healing scaffold relies greatly on the approaches of chemical and biological synthesis, modification, characterisation, including fabrication techniques (Qin et al., 2022). On the other hand, to achieve and stimulate a better healing process, scaffolds play an important role and should consider relevant biochemical and physicochemical features using bioactive materials. Innovation of scaffolds should be based on its ability to: (1) maintain moist conditions; (2) improve epidermal migration by improving blood flow to the wound bed; (3) encourage angiogenesis and connective tissue integration; (4) permit gas exchange between wounded area and surrounding environment; (5) non-toxic, non-adherent to the wound and easy to remove after healing; and (6) should allow debridement action to improve leucocyte migration and assist the accumulation of enzyme (Dhivya et al., 2015; Moura et al., 2017). Taking into consideration all these characteristics, the key features of ideal scaffolds include biocompatibility and bioactivity, porosity, mechanical properties, surface architecture, and degradation.

Several characterisations are adopted to analyse the feature of scaffold. For example, the porosity and interconnectivity can be quantified using techniques such as image analysis of electron microscopy, confocal microscopy, and micro-computed

tomography (micro-CT) (Lombello et al., 2020). Mechanical properties including strength and elasticity are vital for scaffold performance in wound closure and withstanding physiological stresses. Scaffolds need to mimic native tissue mechanics, which can be tested using tensile, compression, or nanoindentation (Negut et al., 2020). Meanwhile, the degradation kinetics are commonly assessed through time-based *in vitro* and *in vivo* degradation studies, employing methods such as measuring mass loss. Surface characterisations also important to identify the surface features and functional groups that promote cellular responses. Techniques such as electron microscopy, atomic force microscopy (AFM), or X-ray photoelectron spectroscopy (XPS) provide insights into surface morphology and chemistry. Scaffold for wound healing require bioactive properties to stimulate tissue regeneration, along with biocompatibility to avoid immune reactions. It can be evaluated using *in vitro* cell culture assays, *in vitro* cytotoxicity tests, and *in vivo* animal studies (Laurano et al., 2022). The general overview characteristics of scaffolds are described in Figure 2.1.

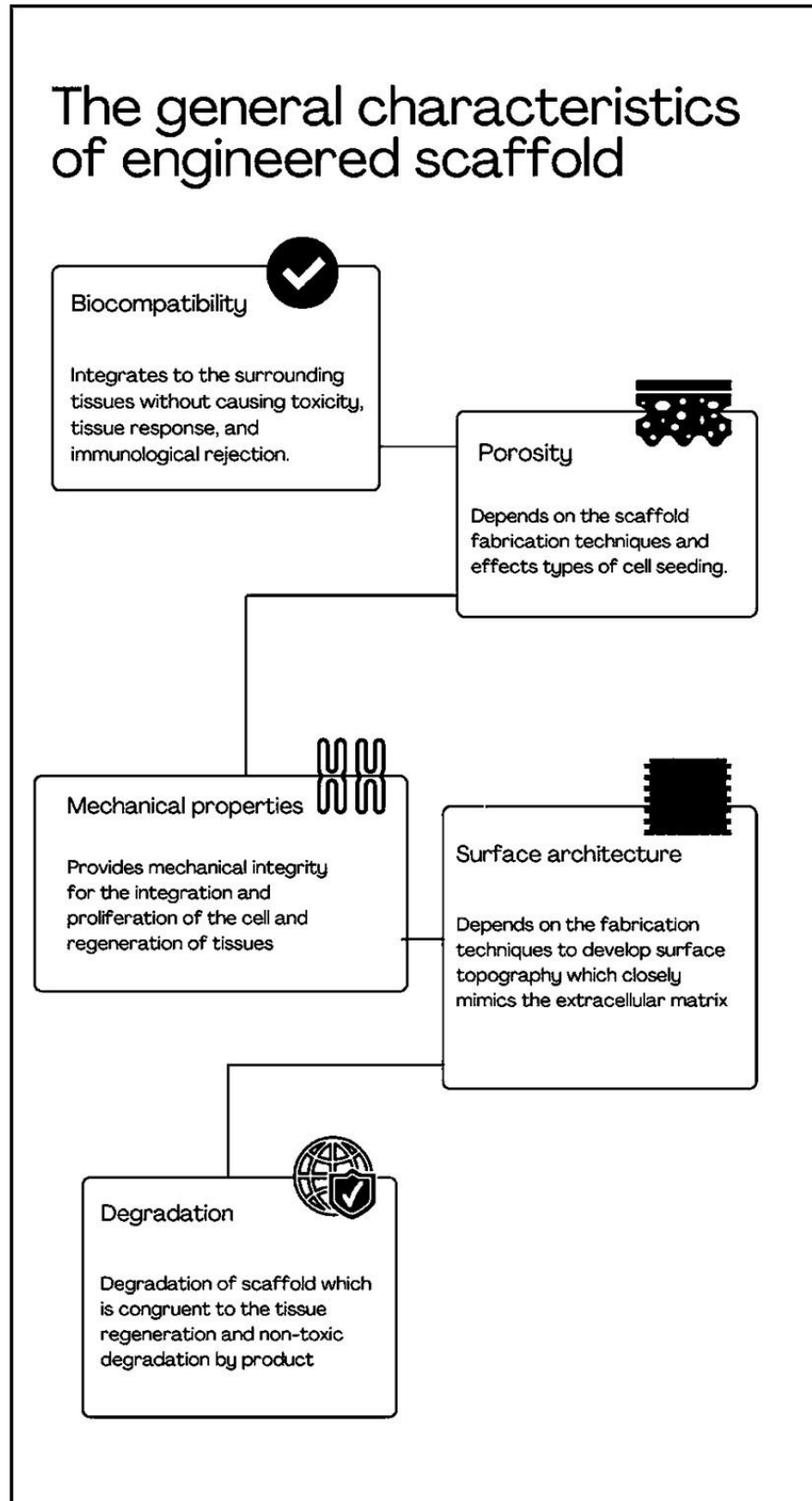


Figure 2.1: The characteristics of engineered scaffold to interact compatibly with biological systems (Adapted from Aiman et al., 2022)

Furthermore, there are various scaffold fabrication methods used for potential wound healing applications, such as solvent casting, electrospinning, 3D-printing, template sponge coating, non-sintering techniques, and freeze-drying techniques. These fabrication methods possess advantages and limitations based on its efficiency and processibility. For example, solvent casting technique is a simple method which can be achieved by dissolving the polymer solution and cast into mould. However, the resulted scaffold might have residual of solvent and poor interconnectivity. The summary of various examples of scaffold fabrication methods are listed in Table 2.1.

Table 2.1: The pros and cons of the various scaffold fabrication techniques used for potential biomedical applications
(Adapted from Aiman et al., 2022)

Types of fabrication	Descriptions	Advantages	Disadvantages	References
Solvent casting and particulate leaching	Involves incorporating water soluble porogen (e.g. NaCl) into polymer suspension and cast into mould where the solvent is removed, porogen are leached out by water or gas foaming to recover a porous structured scaffold.	Straightforward method with controlled pore size through the size of porogen used.	Trace of solvent and porogen particles might be left. Poor mechanical integrity and interconnectivity.	(Majidi et al., 2021; Vigneswari, et al., 2020)
Electrospinning	Production of nano-fibrous scaffold through electric force to draw charged polymer solutions. The diameter of fibres is dependent on the type and concentration of polymer, applied voltage, and flow rate.	Simple operation, fibrous polymer mimics the native ECM structure, and multiple polymers can be combined.	Inconsistent fibres structure which are difficult to control. The overall setup is costly (spinneret and electric supply).	(Azuraini et al., 2019; Vigneswari, et al., 2020)
3D Printing	Methods of designing physical scaffold from 3D digital model (CAD file) into physical form layer by layer materials.	Repeatable and reproducible structure under controlled parameters.	Limited raw material. High cost to setup 3D printer.	(Ghilan et al., 2020; Rastin et al., 2020)

Table 2.1, Continued

Types of fabrication	Descriptions	Advantages	Disadvantages	References
Non-sintering techniques	Super cooled liquids (e.g hydrogen peroxide, sodium phosphate ice) were used to generate bubbles which created pores.	Highly porous.	Low mechanical strength.	(Mehmet O. Aydogdu et al., 2019; Ismadi et al., 2014)
Freeze-drying techniques	Involves sublimation process in which frozen water molecules in the composites scaffolds is directly converted from solid to gas state which pass liquefaction phase.	Inexpensive method as it requires basic laboratory equipment. High porosity and interconnectivity.	The process takes longer period and high energy consumption.	(Singh et al., 2020; Vigneswari et al., 2021)
Template sponge coating	Technique which is typically used for ceramic involves porous sponge template impregnated with slurry and the sintering of the ceramic at high temperature (>1000°C).	Highly interconnected and porous.	Low mechanical strength. High energy consumptions due to high temperature requirement. The architecture of scaffold is dependent on the sponge template.	(Daraei, 2020; X. Tang et al., 2014)

Despite current modalities in the fabrication methods of scaffolds, there are continuous development in understanding the interaction of body with biomaterials. Essentially, surfaces play a key aspect for the development of scaffolds since most biological reactions takes places at the surfaces and interface of the biomaterials when it is exposed to the living organisms (Dave & Gomes, 2019; Kingshott et al., 2011). For instance, the reaction consists of water adsorption at the surface of scaffolds which afterwards draws bioactive molecule adsorption followed by cell attachment to the surface of scaffolds (Vladkova, 2010). Thus, the progress of wound scaffolds by applying biological modification and functionalisation of the biopolymer with bioactive materials has greatly advanced the therapeutic interventions which translate the laboratory research into clinical practices and commercial products.

2.3 Polyhydroxyalkanoate (PHAs): The next generation biopolymer

The medical-engineering multidisciplinary convergence has strongly promoted the progress of PHA in specific and precise tissue repair and regeneration, while providing a new approach for the development of biomedical application. Polyhydroxyalkanoates (PHAs) are also known as poly(4-alkan-2-oxelanonnes) is a group of biopolymers that consists of repeated hydroxyalkanoates monomer. Typically, PHA is one of the significant polymers that displayed biodegradability, biocompatibility and other characteristics resembling synthetic plastics (Doi et al., 1990). Due to this, it has become a significant and one of carbon neutral polymer candidates that can reduce the dependent of mankind toward fossil fuels (Tan et al., 2014). These biopolymers are microbial polyesters, where it is synthesised by various kind of microorganisms as an intracellular carbon and energy reserve under stress condition (Zinn et al., 2001). Various bacterial species from archaebacteria and eubacteria could synthesise PHA (Zinn et al., 2001). This comprises of diverse

bacterial classes of both Gram-negative and Gram-positive represented by *Bacillus* sp., *Streptomyces* sp., *Rhodococcus* sp., *Clostridium* sp., *Staphylococcus* sp., *Corynebacterium* sp., *Nocardia* sp., *Cupriavidus* sp., *Pseudomonas* sp., *Methylobacterium* sp., *Azobacter* sp., *Burkholderia* sp. and recombinant *Escherichia coli* (Liu et al., 2016). Besides that, some bacteria have been shown to synthesise PHA without any nutrient constraint like *Alcaligenes latus strain* IAM 12,664 T (Obruca et al., 2018).

The aggregation of PHA in bacterial cells occurs naturally as the carbon exceed the needs or if other essential nutrients are limited such as oxygen, nitrogen, magnesium, sulphur and phosphate (Anderson & Dawes, 1990; Liu et al., 2016). The biology of PHA granules is a way simpler and functioning as organelle-like inclusion bodies, nano-sized discrete and optically dense granules which bounded in an amorphous state within the cytoplasm of microbial cells (Muhammadi et al., 2015; Sudesh et al., 2000). The PHA granules are mostly spherical and surrounded by a phospholipid membrane separating two crystalline protein layers, which is composed of the PHA polymerases, intracellular PHA depolymerase, amphipathic phasing proteins, PHA-specific regulator proteins and additional proteins with unknown function (Klinke et al., 2000). Although PHAs are stored in the cytoplasm, it does not interrupt the osmotic stress of the cell despite it is present in large amounts. Thus, it prevents the effusion of valued compounds from the cells and enhance physiological performance (Verlinden et al., 2007). Granules membrane coat is about 2 nm thick, containing 0.5% lipid and 2% protein of the granule weight (Lundgren & Pfister, 1964). These PHA granules can be identified phenotypically by specifically stain with Sudan black or light fluorescent stains such as Nile blue and Nile red, which result in dark blue or fluorescent granules (Muhammadi et al., 2015). PHA granules are

observed as light- refracting granules under phase contrast microscope, and as electron transparent, discrete, spherical particles with clear boundaries under transmission microscopic observation (Balakrishnan, 2011).

Hydrogen bonds between carbonyl groups of the individual monomers stabilise the helical structure of PHA-helix in terms of its molecular structure, whereas the monomeric composition of PHA is regulated by a variety factors, including the strain of organisms, the formulation of medium, the bioprocess parameters, and the modes of fermentation, such as continuous, fed-batch, and batch (Koller, 2018). Furthermore, the chemical composition of the PHA is made up of a diverse range of monomers depending on the substrate specificity of PHA synthase of the microorganisms. The primary enzyme in the synthesis of PHA, PHA synthase also controls the size of monomers (Loo & Sudesh, 2007). PHA can be synthesised in the form of homopolyesters, copolyesters, terpolyesters, or polyester blends (Bhatt et al., 2008). To date, there are more than 150 monomers found to be produced by more than 300 microorganisms, with each of the unit's monomer comprised of (*R*)-group side chain that made up of saturated, branched, or substituted alkyl group (Tan et al., 2014). Figure 2.2 shows the general chemical structure of various PHAs. This variation causes PHA to be easily altered to synthesised polymers with distinct properties.

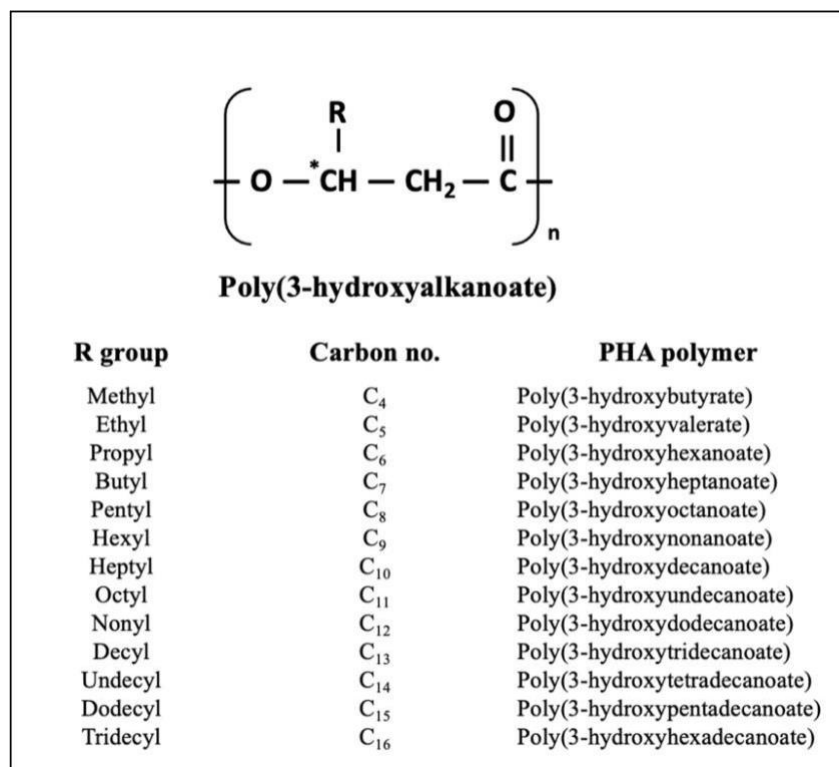


Figure 2.2: Chemical structure of PHA. The functional alkyl represents the nomenclature and number of carbons for PHA compound. Asterisk stands for chiral centre for PHA-building block (Adapted from Tan et al., 2014).

Among the various groups of biopolymers, PHA resembles similar feature to synthetic thermoplastics that are biodegradable and biocompatible. Thus, it is an ideal substitute for the synthetic polymers and make PHA a promising biomaterial product to be applied in biomedical area (Tan et al., 2014). PHAs and their degradation product 3- hydroxyacids have been found in a wide range of organisms, from bacteria to higher mammals (Muhammadi et al., 2015). Upon the *in vivo* degradation of various PHA based biomaterials, the results of these findings report no formation of toxic compounds in the organisms (Martin & Williams, 2003; Zinn et al., 2001). For instance, a company named Tephra Inc based in Cambridge expand the usage of PHA by manufacturing several PHA-based products such as heart valves, sutures, implants, and microparticulate carriers. Among these products, TephraFLEX that is an

absorbable suture from poly(4-hydroxybutyrate) is the pioneer product that has been endorsed by Food and Drug Administration (FDA) (Shrivastav et al., 2013). PHA also known as a pharmaceutically active compound, sparking interest in the development of potential anti-cancer drugs, anti-HIV drugs, antibiotics, and tissue engineering medications (Rai et al., 2011). Some key applications of PHA include the usage as tissue engineering scaffolds since it can be fabricated as porous scaffolds that mimic the extracellular matrix, providing structural support for tissue regeneration. PHA-based films or hydrogels are utilised as wound dressing due to their biocompatibility to promote wound closure, reduce inflammation, and prevent microbial infection. Surgical implants like sutures, screws, plates, and tissue fixation devices provide temporary support and degrade gradually over time, which eliminating the need for implant removal surgery. Overall, PHA's offer promising opportunities in biomedical engineering for the development of biocompatible, biodegradable materials with diverse applications. Meanwhile, the acknowledgement of other hydroxyalkanoates sets a serious blow in PHA commercialisation. Hence, the incorporation of other hydroxyalkanoates into the homopolymer may improve the material properties.

2.3.1 Derivation of polyhydroxyalkanoate

The number of carbon chain and composition of PHA at the hydroxyalkanoates monomer level are mainly depends on the types of bacterial strains, the process of PHA synthesis and their PHA synthases. The novelty on structure of monomers can be established through physical and chemical modification PHAs can be categorised into several classes based on various aspects such as the common is the number of hydroxyalkanoates monomer that are integrated within polymerisation chain. The first category belongs to short chain-length PHA (SCL-PHA) with 3 to 5 carbons, the second category consists of medium chain-length PHA (MCL-PHA) with the range